$$\phi = [(6\lambda N)^{1/3}/6\pi]F_P(T/T_F) \quad (4)$$

For our experimental conditions, $\phi \approx 1.3F_P(T/T_F)$, which is independent of the trap depth as long as $k_F|a_S| \gg 1$. Because F_P is at most of order unity, strongly hydrodynamic behavior arising from collisions seems unlikely. Including the temperature dependence, ϕ ranges from 0.8 down to 0.2 where the system is nearly collisionless. Hence, collisional hydrodynamics does not provide a satisfactory explanation of the observed anisotropic expansion, whereas superfluid hydrodynamics is plausible.

Given this possibility, we have performed an initial investigation of the transition between ballistic and hydrodynamic expansion. We measure the aspect ratio for an expansion time of 0.6 ms as a function of the evaporation time. For short evaporation times < 0.13 s, where $T/T_F > 3.5$, the measured aspect ratio is consistent with that expected for ballistic expansion. For any evaporation time > 1.5 s, the aspect ratio is consistent with hydrodynamic expansion. We observe a very smooth transition between these two extremes. In the intermediate regime, at temperatures below $T/T_F = 3.5$, the expansion lies between hydrodynamic and ballistic. At $T/T_F = 3.5$, where the evaporation time is short and the number is large, an estimate of the classical collision rate with a unitarity-limited cross section shows that the onset of collisional behavior is not surprising. In the intermediate region, there is no theory of expansion to describe the spatial anisotropy of the energy release. Hence, any attempt to determine the temperature is highly model-dependent and cannot be trusted. To further complicate the analysis, varying the evaporation time changes the trap population in addition to the temperature. Finally, if high-temperature resonance superfluidity does exist, the transition temperature is predicted to be in the range 0.25 to 0.5 T_F, where Pauli blocking is not very effective. Hence, one would not expect to observe a collisionless region immediately before the onset of superfluid hydrodynamics, unless the transition occurs at very low temperature, in contrast to predictions.

There are a number of noticeable discrepancies between the hydrodynamic theory and the data. The deviations at 0 and 0.1 ms can be explained by possible index-of-refraction effects as well as spatial resolution limits. These issues are not important for longer expansion times, where the density is reduced and the cloud size is well beyond the resolution limit of our imaging system. However, close examination of the long time deviations reveals that there may be a two-component structure in the gas. In the axial direction, hydrodynamic expansion is very slow, and a second component expanding according to ballistic or collisionless mean field scaling (Fig. 3B) easily overtakes the hydrodynamic component. A two-component structure may also explain why the axial spatial distributions (Fig. 2B) are better fit by Gaussian distributions than by zero-temperature T-F distributions. By contrast, in the transverse direction, the hydrodynamic expansion is the fastest, masking any two-component structure after a short time.

References and Notes

1. P. F. Bedaque, U. van Kolck, available at www.arxiv.org/abs/nucl-th/0203055.
2. W. V. Liu, F. Wilczek, available at www.arxiv.org/abs/cond-mat/0208052.
3. M. Randeria, *Bose-Einstein Condensation*, A. Griffin, D. W. Snoke, S. Stringari, Eds. (Cambridge Univ. Press, Cambridge, 1995), pp. 355–392.
4. H. T. C. Stoof, M. Houbiers, C. A. Sackett, R. G. Hulet, *Phys. Rev. Lett.* **76**, 10 (1996).
5. M. Houbiers *et al.*, *Phys. Rev. A* **56**, 4864 (1997).
6. R. Combescot, *Phys. Rev. Lett.* **83**, 3766 (1999).
7. H. Heiselberg, *Phys. Rev. A* **63**, 043606 (2001).
8. M. Holland, S. J. J. M. F. Kokkelmans, M. L. Chiofalo, R. Walser, *Phys. Rev. Lett.* **87**, 120406 (2001).
9. E. Timmermans, K. Furuya, P. W. Milonni, A. K. Kerman, *Phys. Lett. A* **285**, 228 (2001).
10. Y. Ohashi, A. Griffin, *Phys. Rev. Lett.* **89**, 130402 (2002).
11. S. J. J. M. F. Kokkelmans, J. N. Milstein, M. L. Chiofalo, R. Walser, M. J. Holland, *Phys. Rev. A* **65**, 053617 (2002).
12. B. DeMarco, D. S. Jin, *Science* **285**, 1703 (1999).
13. A. G. Truscott, K. E. Strecker, W. I. McAlexander, G. B. Partridge, R. G. Hulet, *Science* **291**, 2570 (2001).
14. F. Schreck *et al.*, *Phys. Rev. Lett.* **87**, 080403 (2001).
15. S. R. Granade, M. E. Gehm, K. M. O'Hara, J. E. Thomas, *Phys. Rev. Lett.* **88**, 120405 (2002).
16. Z. Hadzibabic *et al.*, *Phys. Rev. Lett.* **89**, 160401 (2002).
17. G. Roati, F. Riboli, G. Modugno, M. Inguscio, *Phys. Rev. Lett.* **89**, 150403 (2002).
18. C. Menotti, P. Pedri, S. Stringari, available at www.arxiv.org/abs/cond-mat/0208150.
19. K. M. O'Hara *et al.*, *Phys. Rev. A* **66**, 041401(R) (2002).
20. M. Houbiers, H. T. C. Stoof, W. McAlexander, R. Hulet, *Phys. Rev. A* **57**, R1497 (1998).
21. S. Jochim *et al.*, *Phys. Rev. Lett.*, in press (available at www.arxiv.org/abs/physics/0207098).
22. T. Loftus, C. A. Regal, C. Ticknor, J. L. Bohn, D. S. Jin, *Phys. Rev. Lett.* **88**, 173201 (2002).
23. G. Modugno *et al.*, *Science* **297**, 2240 (2002).
24. K. Dieckmann *et al.*, *Phys. Rev. Lett.* **89**, 203201 (2002).
25. K. M. O'Hara, M. E. Gehm, S. R. Granade, J. E. Thomas, *Phys. Rev. A* **64**, 051403 (2001).
26. The systematic uncertainty in the number arises from errors in detuning, saturation parameter, and residual optical pumping (which underestimate the true number, as we assume the maximum cross section), as well as errors in the magnification.
27. Y. Kagan, E. L. Surkov, G. V. Shlyapnikov, *Phys. Rev. A* **55**, 18 (1997).
28. Note that the one-dimensional transverse (axial) distributions are obtained by integrating the column density in the axial (transverse) direction.
29. D. A. Butts, D. S. Rokhsar, *Phys. Rev. A* **55**, 4346 (1997).
30. O. J. Luiten, M. W. Reynolds, J. T. M. Walraven, *Phys. Rev. A* **53**, 381 (1996).
31. B. DeMarco, S. B. Papp, D. S. Jin, *Phys. Rev. Lett.* **86**, 5409 (2001).

32. We thank H. Heiselberg and S. Stringari for stimulating correspondence as well as for independently providing us with the release energy formula of Eq. 3. We also thank D. Gauthier for critical reading of the manuscript. Supported by the Chemical Sciences, Geosciences and Biosciences Division of the Office of Basic Energy Sciences, Office of Science, U.S. Department of Energy through a program on the dynamics of ultracold Fermi gases, by NSF through a program on resonance superfluidity, by the Physics Division of the Army Research Office, and by the Fundamental Physics in Microgravity Research program of NASA.

4 October 2002; accepted 31 October 2002
Published online 7 November 2002;
10.1126/science.1079107
Include this information when citing this paper.

Short-Lived Nuclides in Hibonite Grains from Murchison: Evidence for Solar System Evolution

K. K. Marhas,[1] J. N. Goswami,[1*] A. M. Davis[2]

Records of now-extinct short-lived nuclides in meteorites provide information about the formation and evolution of the solar system. We have found excess ^{10}B that we attribute to the decay of short-lived ^{10}Be (half-life 1.5 million years) in hibonite grains from the Murchison meteorite. The grains show no evidence of decay of two other short-lived nuclides—^{26}Al (half-life 700,000 years) and ^{41}Ca (half-life 100,000 years)—that may be present in early solar system solids. One plausible source of the observed ^{10}Be is energetic particle irradiation of material in the solar nebula. An effective irradiation dose of $\sim 2 \times 10^{18}$ protons per square centimeter with a kinetic energy of ≥ 10 megaelectronvolts per atomic mass unit can explain our measurements. The presence of ^{10}Be, coupled with the absence of ^{41}Ca and ^{26}Al, may rule out energetic particle irradiation as the primary source of ^{41}Ca and ^{26}Al present in some early solar system solids and strengthens the case of a stellar source for ^{41}Ca and ^{26}Al.

Pristine early solar system solids recovered from meteorites contain fossil records of several now-extinct short-lived nuclides with half-lives varying from a hundred thousand years to a few tens of millions of years (*1, 2*). Some of these nuclides with short half-lives, such as ^{41}Ca, ^{26}Al, ^{60}Fe [half-life 1.5 million years (My)], and ^{53}Mn (half-life 3.7 My), are considered to be products of stellar nucleosynthesis that were injected into the protosolar cloud before or during its collapse (*1*). However, the possibility that they could be products of interactions of energetic particles with gas and dust in the solar nebula has also been proposed (*3–5*). The recent discovery of now-extinct ^{10}Be in meteorite (*2*) has strengthened this proposal because ^{10}Be is not a product of stellar nucleosynthesis (*6, 7*). Whether energetic particle interactions also produced the other short-lived nuclides that were present in the early solar system has remained a contentious issue (*1, 4, 5, 8, 9*).

It is important to resolve this issue in order to understand the origin and early evolution of the solar system. If these short-lived nuclides are of stellar origin, they may be used as chronometers to infer time scales of early solar system processes (*10*). On the other hand, if they are products of energetic particle interactions taking place in the solar nebula, they provide information on the energetic environment in the early solar system. We report results obtained from an ion microprobe study of fossil records of three short-lived nuclides, ^{41}Ca, ^{26}Al, and ^{10}Be, in a set of selected early solar system solids. These results allow us to put a limit on the energetic particle irradiation of the solar nebula.

[1]Physical Research Laboratory, Ahmedabad 380009, India. [2]Enrico Fermi Institute and Department of the Geophysical Sciences, University of Chicago, Chicago, IL 60637, USA.

*To whom correspondence should be addressed. E-mail: goswami@prl.ernet.in

Hibonite [$CaAl_{12-2x}(Mg_x,Ti_x)O_{19}$], a refractory oxide mineral and one of the earliest condensates to form in a high-temperature solar nebula environment (*11*), is found in trace amounts in some primitive meteorites and was chosen for the present study. Hibonite hosts both stable and radiogenic isotope abundance anomalies (*12, 13*). Two distinct groups of hibonite are present. One group hosts large-magnitude stable isotope abundance anomalies, δ^{48}Ca [values ranging from –56 per mil (‰) to 104‰] and δ^{50}Ti (values ranging from –47‰ to 273‰) (*14*), but these are devoid of evidence for in situ decay of short-lived ^{26}Al and ^{41}Ca. The second group contains fossil records of ^{26}Al and ^{41}Ca and hosts small-magnitude stable isotope anomalies. The grains selected for this study belong to the first group and were identified from a systematic study of ^{26}Al and ^{41}Ca in more than two dozen hibonite crystals recovered from the Murchison carbonaceous chondrite. The analyzed samples include hibonite from a large millimeter-sized hibonite-rich refractory object (SH-7) found on the surface of a broken fragment of this meteorite and individual platy hibonite crystals (CH-B7 and CH-C1) recovered from an acid-resistant residue of another sample of Murchison.

Our data for ^{26}Al in SH-7 and CH-B7 are consistent with data reported earlier (*12, 15*). All three samples show no detectable radiogenic ^{26}Mg from ^{26}Al decay (Table 1), and we can place a 2σ upper limit of 2×10^{-6} for initial ^{26}Al/^{27}Al by combining data for these three hibonite grains. This value is below the canonical early solar system value of 5×10^{-5} for this ratio seen in a large number of CAIs (Ca- and Al-rich inclusions) from different meteorites (*16*). CH-B7 and SH-7 are also devoid of ^{41}Ca (*12, 15*), and we could not detect radiogenic ^{41}K from the decay of ^{41}Ca in CH-C1 (Table 1). These data suggest an upper limit of 3×10^{-9} for initial ^{41}Ca/^{40}Ca at the time of closure of the Ca-K system in these objects that is below the canonical early solar system value of 1.4×10^{-8} for this ratio inferred from studies of a large number of CAIs (*12, 17*). On the other hand, the measured boron isotopic ratios (*18*) in the three hibonite grains provide evidence for excess ^{10}B in them. The measured ^{10}B/^{11}B ratios correlate with the ^{9}Be/^{11}B ratio in the samples (Fig. 1), indicating that the excess ^{10}B is due to in situ decay of ^{10}Be initially present in hibonite (*19*). The data also suggest variation in the initial ^{10}Be/^{9}Be values for the three samples [$\sim 8 \times 10^{-4}$ (CH-B7), $\sim 4 \times 10^{-4}$ (SH-7), and $\sim 1.5 \times 10^{-3}$ (CH-C1)]. If we combine data for the three samples, they yield an average initial ^{10}Be/^{9}Be value of 5.2 ($\pm$2.8) $\times 10^{-4}$ [2σ error (*19*)]. The possibility of differential loss of ^{26}Al and ^{41}Ca (or their daughter products ^{26}Mg and ^{41}K) relative to ^{10}Be (or ^{10}B) in the analyzed hibonite can be ruled out on the basis of the well-preserved large-magnitude stable isotope anomalies in ^{16}O, ^{48}Ca, and ^{50}Ti (*12, 20, 21*). Further, the hibonite grains are characterized by nearly uniform enrichment of the refractory rare earth elements by a factor of ~100 above chondritic (CI meteorite) abundances (*12, 21, 22*) that suggest them to be some of the first-generation solids to form in the solar nebula that were not affected by any secondary processes after for-

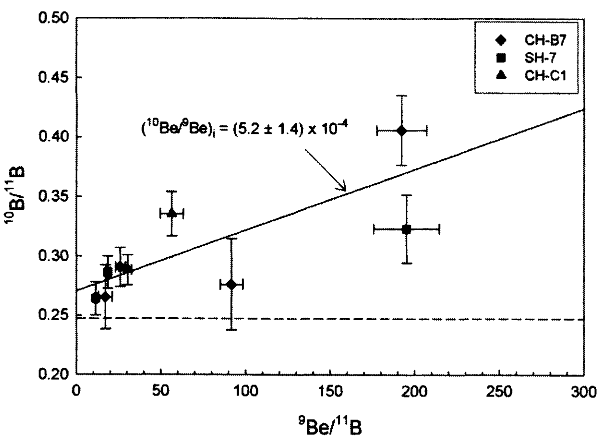

Fig. 1. Be-B isotopic systematics in the three Murchison hibonite samples analyzed in this study. The measured ^{10}B/^{11}B ratios are higher than the normal value (shown by the dashed line) and correlate with ^{9}Be/^{11}B, indicating that the excess in ^{10}B is due to in situ decay of ^{10}Be initially present in the hibonites. The slope of the best-fit line through the data points (the solid line) yields an initial ^{10}Be/^{9}Be ratio of 5.2 (±1.4) × 10^{-4}; the value of the intercept (0.272 ± 0.008) is a measure of initial ^{10}B/^{11}B in the hibonite (*19*). Error bars are 1σ.

Table 1. Be-B, Al-Mg, and Ca-K isotopic composition in Murchison hibonites. The Al-Mg data are based on three measurements each on CH-B7 and SH-7 and one measurement on CH-C1; Ca-K data for CH-B7 are from (*12*) and for SH-7 from (*15*).

Sample	^{9}Be/^{11}B* ($\pm 2\sigma_m$)	^{10}B/^{11}B ($\pm 2\sigma_m$)	^{27}Al/^{24}Mg ($\pm 2\sigma_m$)	^{26}Mg/^{24}Mg ($\pm 2\sigma_m$)	(^{26}Al/^{27}Al)$_i$	^{40}Ca/^{39}K ($\pm 2\sigma_m$)	^{41}K/^{39}K ($\pm 2\sigma_m$)	(^{41}Ca/^{40}Ca)$_i$
CH-B7	17.2 ± 8.2	0.2655 ± 0.0540	103.6 ± 0.1	0.13954 ± 0.00027	<4.7×10^{-6}	2.4(±0.26)×10^{6}	0.070 ± 0.012	<4.2 × 10^{-9}
	26.0 ± 5.8	0.2907 ± 0.0329						
	91.7 ± 13.3	0.2761 ± 0.0771†						
	192.2 ± 29.6	0.4061 ± 0.0584						
SH-7	11.4 ± 1.5	0.2642 ± 0.0280	77.6 ± 0.13	0.13919 ± 0.00025	<1.5×10^{-6}	4.3(±2.1) ×10^{6}	0.073 ± 0.013	<3.3 × 10^{-9}
	18.5 ± 2.8	0.2864 ± 0.0271						
	195.1 ± 38.8	0.3231 ± 0.0574						
CH-C1	30.4 ± 4.3	0.2885 ± 0.0254‡	71.7 ± 0.6	0.13917 ± 0.00042	<3.8×10^{-6}	1.5(±0.11)×10^{6}	0.070 ± 0.008	<4 × 10^{-9}
	56.4 ± 13.6	0.3354 ± 0.0374						

*Be content in the three hibonite grains ranges from 0.4 to 1.6 ppm; variation within individual hibonite ranges from a factor of ~2 (SH-7, CH-C1) to ~4 (CH-B7). †Corrected for possible hydride interference (*18*). ‡Mean of two measurements.

mation. It is also not possible to explain the much lower abundances of ^{26}Al, relative to ^{10}Be, by considering a late formation of the hibonite in the nebula (*23*). These data demonstrate that the source contributing to the observed ^{10}Be in the hibonite did not contribute significant amounts of ^{41}Ca and ^{26}Al.

Energetic particle irradiation of solar nebula or protosolar cloud material could be the source of ^{10}Be present in the hibonite grains. A type II supernova origin of ^{10}Be by spallation reactions induced by the passage of r = process jets (very high velocity outflow from the central neutron star) through the expanding supernova envelope has also been suggested (*24*). However, this model predicts the coupled presence of the nuclides ^{10}Be, ^{41}Ca, and ^{26}Al in early solar system solids and can be ruled out. Galactic cosmic ray (GCR) irradiation of the protosolar cloud could be a viable source of ^{10}Be if the GCR flux had increased by at least a factor of 10 during the 2 to 3 My preceding the collapse of this cloud (*9*). At present, there is no conclusive evidence for such an increase, and this does not appear to be a plausible source of ^{10}Be present in early solar system solids (*9, 25, 26*). Irradiation of gas and dust in the solar nebula by solar energetic particles (SEPs) from an active early Sun is therefore a more likely proposition.

We estimated the effective irradiation dose and characterized the nature of the SEPs by making some simplifying assumptions (*27*). Figure 2 shows the estimated enrichment or depletion in the initial abundances of ^{26}Al and ^{41}Ca (relative to their canonical early solar system values) for two values of the spectral parameter γ, assuming a power law in kinetic energy (E) representation of the SEP flux ($dN/dE \propto E^{-\gamma}$, where N is the number of SEPs), and for irradiation durations of 10 to 10^7 years; in each case, SEP fluence was adjusted such that production of ^{10}Be matches an initial solar system $^{10}Be/^{9}Be$ ratio of $\sim 10^{-3}$ (*2, 28–31*). The most stringent upper limits of initial ^{26}Al and ^{41}Ca abundances inferred from our data for the hibonite grains, relative to their canonical early solar system abundances ($^{26}Al/^{27}Al = 5 \times 10^{-5}$; $^{41}Ca/^{40}Ca = 1.4 \times 10^{-8}$), are also shown in Fig. 2. Steeper energy spectra for the SEPs (e.g., $\gamma \geq 3$) will lead to production of ^{41}Ca above its canonical abundance, whereas depletion in ^{26}Al will be less than a factor of 12 from its canonical abundance. On the other hand, a flatter spectra with $\gamma \leq 2$ will produce ^{41}Ca and ^{26}Al much below their canonical abundance (Fig. 2) while producing the requisite amount of ^{10}Be (*32*). A similar conclusion is reached when we consider an exponential in rigidity (R) representation for the SEP flux [$dN/dR \propto \exp(-R/R_o)$ (*27*)]. Production of ^{41}Ca and ^{26}Al, above the upper limits obtained in this study, can be avoided for relatively flatter spectra with values of R_o exceeding 150 MV (*32*). We estimate the effective irradiation dose received by the nebular material to be $\sim 2 \times 10^{18}$ protons cm^{-2} with energy ≥ 10 MeV amu^{-1}. These estimates are based on a CI chondritic composition of the irradiated nebular matter. If we consider nebular material of refractory composition (e.g., similar to composition of CAI or hibonite), production of ^{26}Al and ^{41}Ca will be higher because of high Al and Ca content (relative to CI chondrites), and it is not possible to identify specific SEP spectral shapes and fluences that will match the observed abundances of ^{10}Be, ^{26}Al, and ^{41}Ca in the analyzed hibonite grains. The spread in the initial $^{10}Be/^{9}Be$ in the hibonite grains may reflect varying doses of SEP irradiation received by the hibonite precursor nebular material as a result of differences in their irradiation condition and duration.

The SEP interaction with nebular material may take place either close to the Sun, in the proposed X-wind irradiation model for durations of a few tens of years (*4, 5, 9*), or in the meteorite-forming zone (2 to 4 AU) in the nebula over an extended period of time. The preference for a steep energy spectrum with $\gamma \sim 4$ in the X-wind model (*9*) makes it inconsistent with our observations. On the other hand, if we consider a longer duration ($\sim 10^5$ years) irradiation of nebular material by SEPs characterized by a relatively flat energy spectrum ($\gamma \sim 2$), the SEP flux from the early Sun at 1 AU must have been higher by a factor of $\sim 10^4$ than the average value of 100 protons cm^{-2} s^{-1} with energy ≥ 10 MeV amu^{-1} for the past few million years inferred from lunar sample studies (*33*). A relatively flat spectrum for SEPs from an active early Sun was also proposed previously to explain the isotopic composition of SEP-produced neon in individual grains of gas-rich meteorites exposed to energetic particles from the early Sun (*34*).

The finding that ^{10}Be is present in Murchison hibonite devoid of ^{41}Ca and ^{26}Al is in marked contrast to the data obtained for CAIs from CV meteorites, which establish that both ^{10}Be and ^{26}Al (and, where data are available, ^{41}Ca) are present in these CAIs (*28–31*). However, the initial $^{10}Be/^{9}Be$ ratios in these CAIs show a spread (5×10^{-4} to 16×10^{-4}) that is similar to that in the hibonite grains analyzed in this study (4×10^{-4} to 15×10^{-4}). Further, the range of Be content (0.2 to 1.5 ppm) in melilite, the mineral phase in CAIs analyzed to look for ^{10}Be records (*2, 28–30*), is also similar to that in the hibonite (Table 1). If we attribute the source of ^{10}Be in both these sets of objects to irradiation of their precursor nebular material by SEPs with the characteristics noted above, we need an additional source for the short-lived nuclides ^{41}Ca and ^{26}Al present in their canonical abundances in the CV CAIs, and a stellar source is the only viable option (*35*). The absence of these nuclides in the Murchison hibonite suggests that these hibonite grains formed in a region within the collapsing protosolar cloud before the arrival of the short-lived radioactivities injected from a stellar source, and they may predate the CAIs from CV meteorites (*12, 36*).

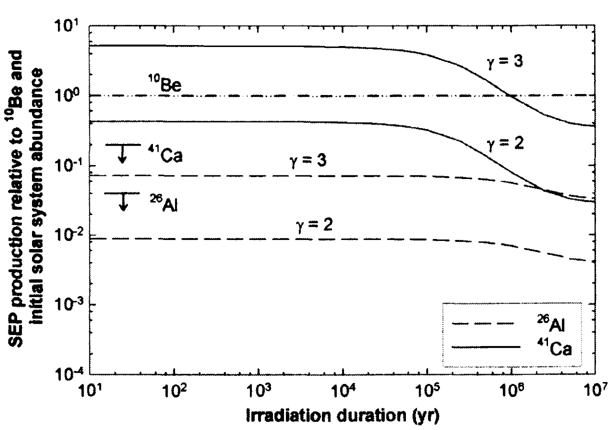

Fig. 2. Production of the short-lived nuclides ^{41}Ca (solid line) and ^{26}Al (dashed line), relative to ^{10}Be, by SEPs for different spectral parameters (γ = 2 and 3) in the power-law representation of the SEP spectrum, $dN \propto E^{-\gamma}dE$ (*27*) as a function of irradiation duration. The targets are assumed to be spherical and CI chondritic in composition, with sizes varying from 10 μm to 1 cm and following a power-law size distribution ($dn/dr \propto r^{-4}$). The SEP flux is adjusted to match ^{10}Be production with an initial $^{10}Be/^{9}Be$ ratio of 10^{-3} (represented by the dashed-dot line). The values for solar system initial $^{26}Al/^{27}Al$ and $^{41}Ca/^{40}Ca$ are taken as 5×10^{-5} and 1.4×10^{-8}, respectively (*16, 17*). The drop in production of ^{41}Ca and ^{26}Al, relative to ^{10}Be, for irradiation durations exceeding 1.5×10^5 and 10^6 years, respectively, reflects the effect of saturation in production of these nuclides, as the irradiation duration exceeds their mean lives. The upper limits of ^{26}Al and ^{41}Ca abundances in the analyzed hibonite are also shown.

References and Notes

1. J. N. Goswami, H. A. T. Vanhala, in *Protostars and Planets IV*, V. Mannings, S. S. Russell, A. P. Boss, Eds. (Univ. of Arizona Press, Tucson, AZ, 2000), pp. 965–996.
2. K. D. McKeegan, M. Chaussidon, F. Robert, *Science* **289**, 1245 (2000).
3. D. Heymann, M. Dziczkaniec, *Science* **191**, 79 (1976).
4. F. H. Shu, H. Shang, A. E. Glassgold, T. Lee, *Science* **277**, 1475 (1997).
5. T. Lee, F. H. Shu, H. Shang, A. E. Glassgold, K. E. Rehm, *Astrophys. J.* **506**, 898 (1998).
6. The light elements Li, Be, and B are readily destroyed in high-temperature nuclear burning in stellar interiors. They are considered to be products of interactions of energetic particles in interstellar space with ambient interstellar matter [see, e.g. (*7*)].
7. H. Reeves, *Rev. Mod. Phys.* **66**, 193 (1994).
8. J. N. Goswami, K. K. Marhas, S. Sahijpal, *Astrophys. J.* **549**, 1151 (2001).
9. M. Gounelle, F. H. Shu, H. Chang, A. E. Glassgold, K. E. Rehm, T. Lee, *Astrophys. J.* **548**, 1051 (2001).
10. It is possible to estimate the time between the ejection of short-lived radioactivities from a stellar source (such

as a supernova or a thermally pulsing asymptotic giant branch star or a Wolf-Rayet star) and the formation of some of the early solar system objects in which their records are found by considering stellar nucleosynthesis yields and a suitable model for transport into and subsequent mixing of the radioactivities with the protosolar cloud [e.g. (1)]. If a homogeneous distribution of the short-lived nuclides in the solar nebula is assumed, they may be used as relative chronometers for dating solar system events and processes.

11. S. Yoneda, L. Grossman, *Geochim. Cosmochim. Acta* **59**, 823 (1995).
12. S. Sahijpal, J. N. Goswami, A. M. Davis, *Geochim. Cosmochim. Acta* **64**, 1989 (2000).
13. T. R. Ireland, *Geochim. Cosmochim. Acta* **54**, 3219 (1990).
14. The symbol δ is used to represent the magnitude of abundance anomaly in a given isotope with respect to a reference isotope. In the case of ^{48}Ca and ^{50}Ti, the reference isotopes are ^{44}Ca and ^{48}Ti, respectively. In general, the abundance anomaly in a given isotope can be expressed as $\delta^iM = \{[(^iM/^jM)_{sample}/(^iM/^jM)_{standard}] - 1\} \times 1000‰$, where *j* represents the reference isotope. A suitable standard with normal isotopic composition is used to infer the magnitude of the anomaly.
15. S. Sahijpal, J. N. Goswami, A. M. Davis, L. Grossman, R. S. Lewis, *Nature* **391**, 559 (1998).
16. G. J. MacPherson, A. M. Davis, E. K. Zinner, *Meteoritics* **30**, 365 (1995).
17. G. Srinivasan, S. Sahijpal, A. A. Ulyanov, J. N. Goswami, *Geochim. Cosmochim. Acta* **60**, 1823 (1996).
18. Samples were analyzed with a Cameca ims-4f ion microprobe at the Physical Research Laboratory, Ahmedabad. Techniques are described in supplemental data on *Science* Online.
19. The correlation between the excess in the daughter nuclide abundance and the abundance of a stable nuclide of the parent element (^{10}B and ^{9}Be in the present case), relative to a suitable normalizing isotope (^{11}B), suggests that the excess is due to in situ decay of the parent nuclide (^{10}Be). The measured isotopic abundance ratio of the boron isotopes can be expressed as $(^{10}B/^{11}B)_m = (^{10}B/^{11}B)_i + [(^{10}Be/^9Be)_i \times (^9Be/^{11}B)_m]$, where the subscripts m and i denote measured and initial, respectively. In obtaining the value of $(^{10}Be/^9Be)_i$ in the analyzed hibonite, we have not corrected for the amount of stable ^{9}Be produced along with radioactive ^{10}Be during energetic particle irradiation of nebular material. This is justified because of the production ratio of ~0.1 for ^{10}Be/^{9}Be, which can account for only a few percent of ^{9}Be measured in the hibonite; furthermore, the correction would be much smaller than the uncertainties introduced by the errors in the measured ^{9}Be/^{11}B and ^{10}B/^{11}B ratios (Table 1). We used the Isochron program (37) to analyze the data. For obtaining initial $(^{10}Be/^9Be)_i$ for individual hibonite, we assume normal B composition ($^{10}B/^{11}B = 0.2473$) in them; no such assumption was made while analyzing the combined data set (Fig. 1).
20. J. N. Goswami, K. D. McKeegan, K. K. Marhas, N. Sinha, A. M. Davis, *Lunar Planet. Sci.* **XXXII**, 1576 (2001).
21. K. K. Marhas, thesis, Devi Ahilya University, Indore, India (2001).
22. A. Hashimoto, R. W. Hinton, A. M. Davis, L. Grossman, T. K. Mayeda, R. N. Clayton, *Lunar Planet. Sci.* **XVII**, 317 (1986).
23. If a time delay is introduced between the production of the short-lived nuclides and the formation of solids in the solar nebula into which they became incorporated, their abundances will be depleted because of free decay; the depletion factor will depend on the time delay and half-lives of the nuclides, with maximum depletion for the shortest lived nuclide. However, a decay interval cannot explain the differences between the initial ^{10}Be and ^{26}Al abundances in the hibonite (Table 1) and their canonical early solar system values ($^{10}Be/^9Be \sim 10^{-3}$ and $^{26}Al/^{27}Al = 5 \times 10^{-5}$).
24. A. G. W. Cameron, *Astrophys. J.* **562**, 456 (2001).
25. Low-energy particle irradiation of the protosolar cloud before or during its collapse, leading to production of isotopes of Li, Be, and B as well as several short-lived nuclides (^{41}Ca, ^{26}Al, ^{53}Mn), was considered as a distinct possibility (38) after the reported observation of enhanced flux of gamma rays from the Orion star-forming region that was suggestive of the presence of a high flux of low-energy particles in star-forming molecular cloud complexes. However, a later reanalysis of the same data set showed that the earlier observation and inferences were erroneous (26). One of the reviewers suggested that a linear increase in metallicity over the lifetime of our galaxy may bring down the required enhancement of GCR flux needed to account for the observed ^{10}Be, and therefore this possibility cannot be ruled out. However there is neither any rigorous published work nor any general consensus on this issue at present.
26. H. Bleomen *et al.*, *Astrophys. J.* **521**, L137 (1999).
27. We consider an active early Sun as the source of the SEPs and represent them using the conventional power law in *E*, $dN/dE \propto E^{-\gamma}$, and exponential in *R*, $dN/dR \propto \exp(-R/R_o)$. We use a set of values for the power-law exponent γ (2 to 5) and for the characteristic rigidity R_o (50 to 400 MV) that cover the range seen in contemporary solar flares. The integral flux of protons above 10 MeV amu^{-1} was normalized to a fixed value in each case. Both proton-induced and α particle–induced reactions were taken into account assuming an α-to-proton ratio of 0.1. We consider irradiation of nebular solids of CI chondritic composition representing precursors of early solar system objects such as hibonite grains and CAIs. The targets were assumed to be spherical, with sizes varying from 10 μm to 1 cm, and to be characterized by a power-law size distribution of the type $dn/dr \propto r^{-\beta}$ (where *n* is the number and *r* is the radius of the targets), with β values of 3 to 5. We ignore possible shielding of the targets by nebular gas and assume free access of SEPs up to the asteroidal zone. Appropriate reaction cross sections for relevant reactions have been used in these calculations (38, 39).
28. K. D. McKeegan *et al.*, *Lunar Planet. Sci.* **XXXII**, 2175 (2001).
29. G. J. MacPherson, G. R. Huss, A. M. Davis, *Geochim. Cosmochim. Acta*, in press.
30. N. Sugiura, Y. Shuzou, A. Ulyanov, *Meteorit. Planet. Sci.* **36**, 1397 (2001).
31. G. Srinivasan, *Meteorit. Planet. Sci.* **36**, A195 (2001).
32. The effective production of ^{10}Be needs high-energy (>50 MeV) protons, whereas ^{41}Ca and ^{26}Al are mainly produced by low-energy (<30 MeV) particles [see (39, 39)]. This difference makes SEP production of ^{10}Be, relative to ^{41}Ca and ^{26}Al, sensitively dependent on the spectral parameters. For a given flux normalization, production of ^{10}Be will increase as the energy spectrum becomes flatter [decreasing value of γ or increasing value of R_o (27)], whereas the reverse is the case for ^{41}Ca and ^{26}Al.
33. R. C. Reedy, *Proc. Indian Acad. Sci.* (*Earth Planet. Sci.*) **107**, 433 (1998).
34. M. W. Caffee, C. M. Hohenberg, T. D. Swindle, J. N. Goswami, *Astrophys. J.* **313**, L31 (1987).
35. Irradiation of different parcels of solar nebula material of varying composition by SEPs with different characteristics can lead to production of the three nuclides (^{26}Al, ^{41}Ca, and ^{10}Be) and provide source material from which CAIs from CV meteorites hosting these nuclides may have formed. However, it is not possible to match the initial solar system abundances of these nuclides unless ad hoc target compositions are considered [see, e.g., (8, 9, 29)]. Further, the observation of variable ^{10}Be/^{9}Be ratios in these CAIs with close to canonical ^{26}Al/^{27}Al ratios cannot be explained in this scenario.
36. S. Sahijpal, J. N. Goswami, *Astrophys. J.* **509**, L137 (1998).
37. A. Provost, *Chem. Geol.* **80**, 85 (1990).
38. R. Ramaty, B. Kozlovsky, R. E. Lingenfelter, *Astrophys. J.* **456**, 525 (1996).
39. J. N. Sisterson, K. Kim, M. W. Caffee, M. Imamura, R. C. Reedy, *Lunar Planet. Sci.* **XXVIII**, 1329 (1997).
40. We thank E. Olsen for sample SH-7, R. S. Lewis for the acid-resistant residue of Murchison, and M. Chaussidon for the GB4 standard (18). Supported by the Department of Space, India (K.K.M., J.N.G.) and by NASA grant NAG5-9510 (A.M.D.).

Supporting Online Material
www.sciencemag.org/cgi/content/full/298/5601/2182/DC1
Materials and Methods

10 September 2002; accepted 6 November 2002

A Late Triassic Impact Ejecta Layer in Southwestern Britain

Gordon Walkden,[1*] Julian Parker,[1] Simon Kelley[2]

Despite the 160 or so known terrestrial impact craters of Phanerozoic age, equivalent ejecta deposits within distal sedimentary successions are rare. We report a Triassic deposit in southwestern Britain that contains spherules and shocked quartz, characteristic of an impact ejecta layer. Inter- and intragranular potassium feldspar from the deposit yields an argon-argon age of 214 ± 2.5 million years old. This is within the age range of several known Triassic impact craters, the two closest of which, both in age and location, are Manicouagan in northeastern Canada and Rochechouart in central France. The ejecta deposit provides an important sedimentary record of an extraterrestrial impact in the Mesozoic that will help to decipher the number and effect of impact events, the source and dynamics of the event that left this distinctive sedimentary marker, and the relation of this ejecta layer to the timing of extinctions in the fossil record.

Major bolide impacts produce craters that may survive long after associated ejecta deposits have been lost through erosion or diagenetic alteration. There are five known late Triassic impact craters (*1*), including the 100-km-diameter Manicouagan crater (Fig. 1), which is one of the largest known Phanerozoic impacts (*2*). Earth experienced a series of worldwide extinctions in the late Triassic, constituting one of the top five Phanerozoic faunal crises (*3*, *4*), but the exact causes are disputed. The discovery of an ejecta deposit corresponding to one or more of these impact

[1]Department of Geology and Petroleum Geology, Kings College, University of Aberdeen, Aberdeen AB24 3UD, UK. [2]Department of Earth Sciences, Open University, Milton Keynes MK7 6AA, UK.

*To whom correspondence should be addressed. E-mail: spherules@abdn.ac.uk